Two Years at Meridiani Planum: Results from the Opportunity Rover

S. W. Squyres,[1] A. H. Knoll,[2] R. E. Arvidson,[3] B. C. Clark,[4] J. P. Grotzinger,[5] B. L. Jolliff,[3] S. M. McLennan,[6] N. Tosca,[6] J. F. Bell III,[1] W. M. Calvin,[7] W. H. Farrand,[8] T. D. Glotch,[9] M. P. Golombek,[9] K. E. Herkenhoff,[10] J. R. Johnson,[10] G. Klingelhöfer,[11] H. Y. McSween,[12] A. S. Yen[9]

The Mars Exploration Rover Opportunity has spent more than 2 years exploring Meridiani Planum, traveling ~8 kilometers and detecting features that reveal ancient environmental conditions. These include well-developed festoon (trough) cross-lamination formed in flowing liquid water, strata with smaller and more abundant hematite-rich concretions than those seen previously, possible relict "hopper crystals" that might reflect the formation of halite, thick weathering rinds on rock surfaces, resistant fracture fills, and networks of polygonal fractures likely caused by dehydration of sulfate salts. Chemical variations with depth show that the siliciclastic fraction of outcrop rock has undergone substantial chemical alteration from a precursor basaltic composition. Observations from microscopic to orbital scales indicate that ancient Meridiani once had abundant acidic groundwater, arid and oxidizing surface conditions, and occasional liquid flow on the surface.

The Mars Exploration Rover Opportunity landed at Meridiani Planum on 24 January 2004. During its 90-sol (martian solar day) nominal mission (*1*), Opportunity explored Eagle crater and the surrounding plains, studying laminated sulfate-rich sandstones that contain abundant hematite-rich spherules (*2*). Opportunity then spent nearly a year exploring Endurance crater, investigating ~7 m of exposed stratigraphic section in a unit dubbed the Burns formation (*3*). Observations there revealed chemical and textural changes with depth (*4*, *5*) and a stratigraphic section dominated by eolian dune and sand sheet facies but with evidence for subaqueous deposition in the uppermost half meter (*6*). Since leaving Endurance, Opportunity has traveled nearly 5 km to the south, assessing horizontal and vertical variations in geology over more regional scales. Major landmarks along the route (fig. S1) include Vostok crater, about 1.5 km south of Endurance, and Erebus crater, about 4 km south of Endurance. Pausing during the traverse, Opportunity also spent considerable time at the Olympia outcrop, just north of Erebus. Despite the generally homogeneous appearance of Meridiani Planum from orbit, a number of new features and phenomena have been observed at these locations at rover scale. Here, we present geologic results obtained along the traverse, interpretations of textural and geochemical observations at Endurance crater, and a refined model for the formation of the sedimentary rocks at Meridiani Planum.

Depositional processes. Rocks of the Burns formation are finely stratified sandstones. By itself, this observation could be explained in terms of eolian or subaqueous sedimentation, accumulation by explosive volcanism, or emplacement as impact ejecta. On the basis of sedimentary structures and facies associations at Eagle (*2*) and Endurance (*6*) craters, we identified eolian and subaqueous sedimentation as the most probable deposition mechanisms.

It is well known that fine- to medium-grained sand, when subjected to shear stresses created by shallow, subaqueous flows with moderate current velocities, spontaneously forms highly sinuous-crested ripples with amplitudes of up to a few cm (*7*, *8*). In cross sections oriented transverse to flow, exposed laminae have a trough-shaped or "festoon" geometry (*9*). At the Olympia outcrop, Panoramic Camera (Pancam) (*10*) images of the rock Overgaard show a planar-laminated unit overlain by the best example of cm-scale trough cross-lamination found by Opportunity to date (Fig. 1A). These trough cross-laminae scour down into the underlying planar laminated unit from left to right. The trough cross-lamination forms a bed set with at least 3 to 4 cm of apparent thickness. Several superimposed sets show basal scouring and backfilling by concave- to occasionally convex-upward cross-laminae, which show a cross-cutting relation in which each trough-shaped subset truncates the subset to its left. In addition, the cross-strata exhibit a small angle of climb from left to right. Truncation surfaces and backfilling of subjacent sets are well expressed in the left-center part of the upper unit. Individual troughs are 3 to 4 cm wide. This particular type of cross-stratification can be further described as scalloped cross-lamination, which can form either by migration of a single bedform during fluctuating flow or by migration of superimposed bedforms in steady flow (*11*). We cannot distinguish between these two possibilities because of the lack of a complementary cut oriented parallel to the bedding plane.

A mosaic of Microscopic Imager (MI) (*12*) images was acquired to provide improved resolution of the Overgaard trough cross-lamination (Fig. 1B). The subgrain-scale resolution of this image provides additional supporting detail, including clear truncation of laminae that reinforces the Pancam observations. Stratal truncations of this sort are the result of primary discontinuities in sedimentation and cannot be artifacts produced by the intersection of bedding with topography. Moreover, fine-scale topography derived from stereoscopic MI imaging reveals a nearly flat surface for the portion of the outcrop that contains the trough cross-lamination. Because there is no systematic relationship of bedding to local slopes, this observation confirms that the cross-lamination is a primary attribute of the rock.

Cross-lamination of this type and at this scale is known to form subaqueously but is not known to develop in other types of flows, including eolian and volcanic base surges (*13*–*15*). We therefore discount suggestions that the Meridiani sandstones might have been formed as a part of volcanic (*16*) or impact (*17*) base surges. Furthermore, the overall stratigraphy and the succession of facies observed at Endurance crater are inconsistent with base surge deposits (*6*). The latter are characterized by flow deceleration sequences similar to subaqueous turbidites (*15*), and these have not been observed in the bedrock at Meridiani. Recent observations thus confirm the earlier interpretation of subaqueous transport and suggest that water flow was more extensive across the ancient Meridiani surface than was evident from observations at Eagle and Endurance craters alone.

Microscopic images provide additional information for testing depositional models. All outcrops imaged to date by Opportunity consist of medium-size sand grains that are rounded and well sorted. For example, Cobble Hill, a target within the interpreted eolian sand sheet facies in Endurance crater, has a mean grain size of 450 μm, with a standard deviation of 170 μm (N = 200) (Fig. 2A). Walker (*18*) and Sparks (*19*) compiled grain-size distribution data for more than 300 pyroclastic flow deposits on Earth. The median grain size in Meridiani outcrops falls within the range of

[1]Department of Astronomy, Space Sciences Building, Cornell University, Ithaca, NY 14853, USA. [2]Botanical Museum, Harvard University, Cambridge, MA 02138, USA. [3]Department of Earth and Planetary Sciences, Washington University, St. Louis, MO 63031, USA. [4]Lockheed Martin Corporation, Littleton, CO 80127, USA. [5]Division of Geological and Planetary Sciences, California Institute of Technology (Caltech), Pasadena, CA 91125, USA. [6]Department of Geosciences, State University of New York, Stony Brook, NY 11794, USA. [7]Geological Science, University of Nevada Reno, Reno, NV 89557, USA. [8]Space Science Institute, Boulder, CO 80301, USA. [9]Jet Propulsion Laboratory, Caltech, Pasadena, CA 91109, USA. [10]U.S. Geological Survey, Flagstaff, AZ 86001, USA. [11]Institut für Anorganische und Analytische Chemie, Johannes Gutenberg Universität, 55099 Mainz, Germany. [12]Department of Earth and Planetary Sciences, University of Tennessee, Knoxville, TN 37996, USA.

medians recorded for terrestrial samples, but the sorting is distinctly different (*20*). In contrast, the size distribution of Meridiani sand grains falls well within the range of mean, median, and sorting values for terrestrial eolian sands (*21*).

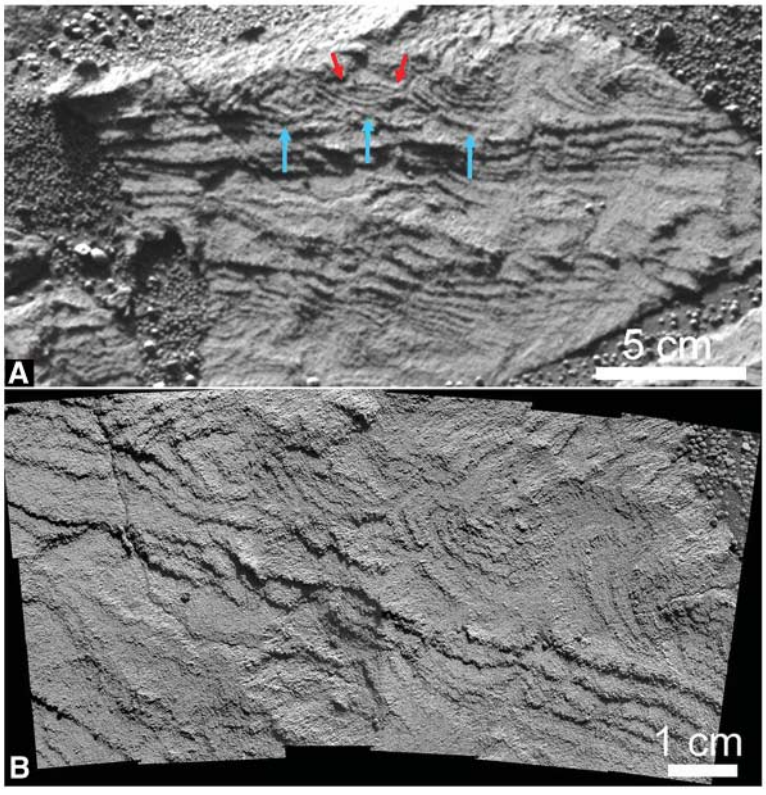

Fig. 1. Festoon (trough) cross-lamination in Overgaard. (**A**) Blue arrows point to three distinct festoons, indicated by basal truncation and concave-upward geometry. Red arrows point to downlapping, convex-up laminae that backfilled the festoon trough. (**B**) MI mosaic of part of Overgaard, showing generally granular texture and excellent sorting, right-to-left pinch out of planar-laminated unit, and stratal truncation and downlap of overlying festoon cross-laminae [compare with (A)]. Illumination is from the top in both images.

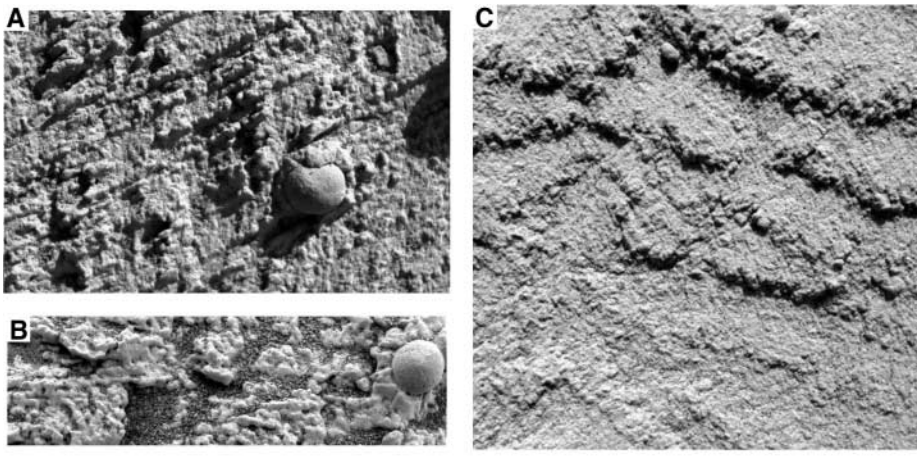

Fig. 2. Microscopic images of Meridiani outcrop rocks. (**A**) Rounded sand grains forming single-grain-thick laminae in target Cobble Hill, an interpreted eolian sand sheet within the measured stratigraphic section in Endurance crater. (**B**) Recrystallization textures in Eagle crater. At center left, a set of three or four laminae show fusing of grains. At right, the complete loss of primary fabric and development of blocky, interlocking crystals around a hematitic spherule implies a highly soluble precursor mineral assemblage. (**C**) Overgaard. Note the absence of visible spherules. Scale across each image is 3 cm.

This characteristic persists south of Endurance crater. Textures in Overgaard, and also in Strawberry, another outcrop near the rim of Erebus crater, again indicate only well-sorted, medium-grained sandstones. Grain-size distributions in sandstones near Erebus approximate those in Eagle and Endurance outcrops (Fig. 2C). Thus, outcrop-level sedimentary structures and fine-scale textures of Meridiani rocks both support the interpretation that they are eolian deposits, reworked locally by surface water.

Geochemistry and mineralogy. After using Opportunity's Rock Abrasion Tool (RAT) (*22*) to expose fresh rock surfaces, we collected Alpha Particle X-Ray Spectrometer (APXS) (*23*) data at Endurance crater that revealed systematic stratigraphic variations in chemical composition (*4*). From bottom to top of the measured stratigraphic section, Burns formation sandstones show decreasing amounts of Si, Al, Na, and K and increasing amounts of Mg and S. This trend is consistent with variations in the ratio of siliciclastic components to sulfates, with the fraction of siliciclastics decreasing upsection. The variations also correlate with diagenetic textural changes, including increased cementation and recrystallization and enhanced secondary porosity deeper in the section (*5*), and accordingly are inferred to result from postdepositional dissolution and mobilization of soluble salts (*4*).

Analysis of these chemical variations sheds light on the nature of the siliciclastic component (Fig. 3). The data form a curvilinear trend with samples from higher in the stratigraphic section plotting at lower $Al_2O_3/(FeO_T + MgO + CaO)$. The two mixing lines in the figure each have one endmember defined by the average composition of "chemical constituents," including sulfate salts, jarosite, and hematite, as inferred from Mössbauer spectroscopy (*24*) and chemical mass balance (*4*, *5*). The deviation of the data from any mixing line, like the lower one, that has unaltered martian basalt as the other endmember shows that the siliciclastic component in the current outcrop cannot be unaltered basalt.

The chemically altered basalt endmember composition for the upper mixing line was derived by assuming that roughly half of the divalent cations were removed from the precursor basalt during chemical weathering, enriching Al in the siliciclastic residue relative to Mg, Fe, and Ca. Deriving it in this way simulates the most important geochemical processes causing Al enrichment relative to divalent cations during chemical weathering of basalt: mineral dissolution and the precipitation of aluminosilicate phases. This mixing line coincides very closely to the Burns formation data. The best fit is found when ~55% of the total Mg, Fe, and Ca is removed (mostly Mg) and is consistent with the siliciclastic component being derived from chemical alteration of a precursor basalt. Further support for the idea

that the siliciclastic component is highly altered comes from Mini–Thermal Emission Spectra (TES) (*25*) infrared data, which show no pyroxene or olivine in the outcrop. Instead, a major component (~25%) of Al-rich amorphous silica is the dominant outcrop spectral signature along with sulfates.

It has been suggested on the basis of limited data from Eagle crater that simple sulfur addition (as H_2SO_4) to basalt with subsequent isochemical alteration might explain the chemistry and mineralogy of the Burns formation (*16*). This explanation would be consistent with geochemical data if all the points were clustered at a single location in Fig. 3, but the trend at Endurance crater rules it out. A mixing line involving addition of sulfur to basalt is a horizontal line on Fig. 3, clearly inconsistent with the trend. Addition of S to basalt could account for the trend only if the primary basaltic sediment composition varied considerably and systematically through the 7 m of stratigraphy exposed in Endurance crater and if the amount of S added varied directly with the primary basaltic composition, an implausible combination of coincidences.

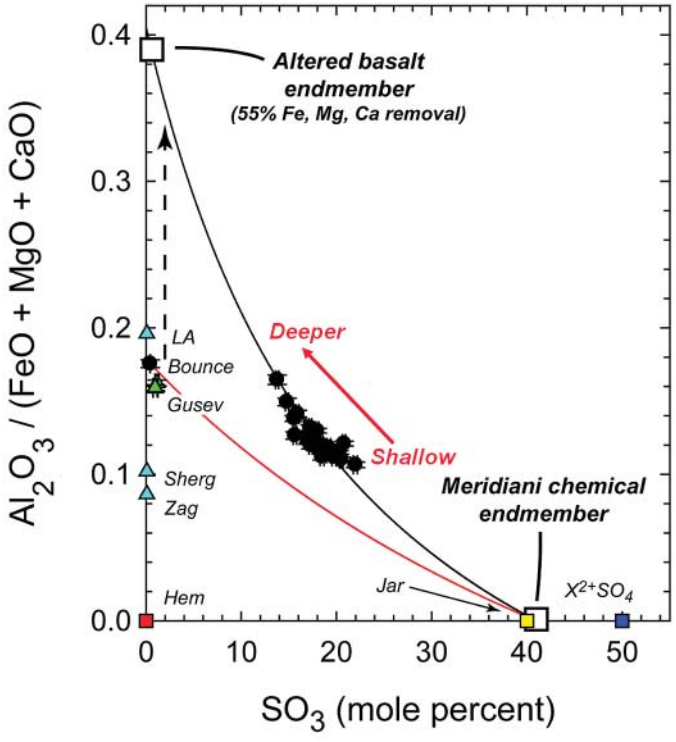

Fig. 3. Plot of molar $Al_2O_3/(FeO_T + MgO + CaO)$ versus SO_3 for the Burns formation (circles). [We sum the three major divalent cations to capture as much of the relevant geochemistry as possible in a single diagram, but we note that most of the observed variability in $Al_2O_3/(FeO_T + MgO + CaO)$ is due to variations in Al_2O_3 and MgO (*4*).] Also plotted are the compositions of martian basalts ("Zag," "Sherg," and "LA" denote the basaltic shergottite meteorites Zagami, Shergotty, and Los Angeles, respectively; "Bounce" denotes Bounce Rock, a piece of impact ejecta at Meridiani Planum (*1*); and "Gusev" denotes plains basalts at Gusev crater), the compositions of minerals observed within the Burns formation ("Hem" denotes hematite and "Jar" denotes jarosite), and a composition derived by removing 50% of the divalent cations (Ca, Mg, and Fe) from typical martian basalt to illustrate the effects of chemical weathering. SO_3 decreases and $Al_2O_3/(FeO_T + MgO + CaO)$ increases systematically with depth (red arrow), indicating an increasing proportion of the siliciclastic component with depth. Also shown are two mixing lines, one between average chemical constituents and unaltered basalt and a second between average constituents and altered basalt.

Diagenesis. Textural evidence for a fluctuating groundwater table in the Burns formation includes (*2*, *5*, *6*) (i) syndepositional sediment deformation, (ii) intergranular cement, (iii) mm-scale spherules interpreted to be concretions, (iv) mm-scale tabular pores interpreted to be crystal molds, (v) late generations of cement and recrystallization surrounding concretions (Fig. 2B), and (vi) decimeter-scale stratigraphically controlled zones of enhanced secondary porosity and recrystallization. As Opportunity traversed south, some features have changed and new textures have been observed.

At Eagle and Endurance craters, crystal molds represent the former presence of mineral grains with solubility comparable to magnesium sulfates, because they dissolved to form secondary porosity without seriously disrupting primary fabrics. Monoclinic habits suggest minerals such as melanterite ($Fe^{2+}SO_4 \cdot 7H_2O$) or calcium, iron, or magnesium chlorides.

North of Erebus crater, the rock Lemon Rind contains pseudomorphs after a mineral with an apparent cubic crystal habit (Fig. 4A). Millimeter-scale square, rectangular, and triangular shapes may suggest the former presence of "hopper crystals" commonly produced by halite in terrestrial evaporites (*26*, *27*). Hopper textures develop in cubic crystals because of preferred growth at edges and corners. They form in many evaporative settings (for example, brine-atmosphere and sediment-brine interfaces and capillary zones), but isolated hoppers within sediment suggest displacive growth above a groundwater capillary fringe (*26*, *28*), similar to the setting inferred for monoclinic-shaped crystal mold minerals (*5*).

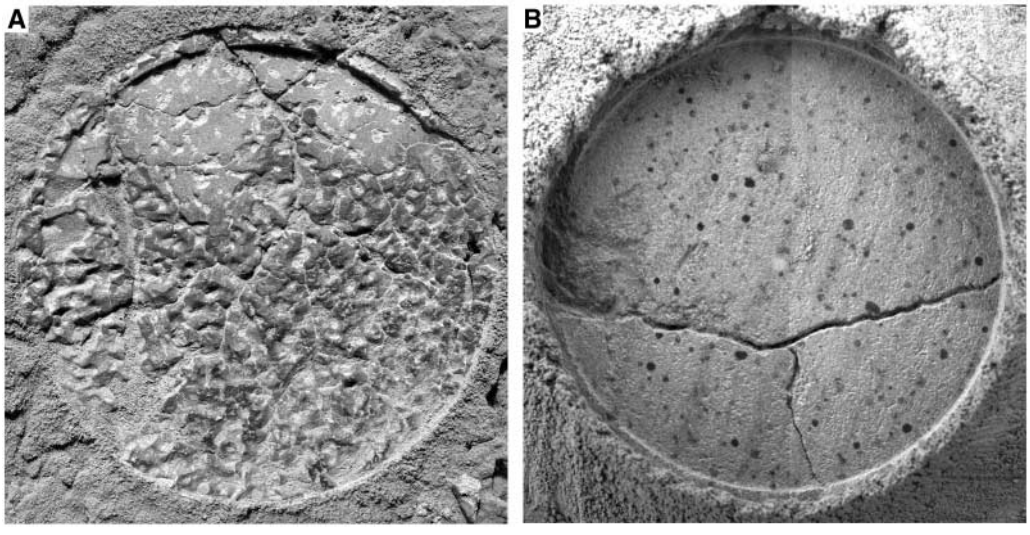

Fig. 4. MI mosaics of RAT holes that reveal diagenetic features observed only south of Endurance crater. (**A**) Apparent pseudomorphs after a mineral with a cubic crystal structure, perhaps halite, in the target Lemon Rind (see Fig. 5A for context). (**B**) Small, irregularly shaped hematite spherules in the target Kalavrita, at the Olympia outcrop. This RAT hole has also exposed a fracture intersection that is part of a polygonal fracture network. Scale across each image is 5 cm.

Within Eagle and Endurance craters, hematitic spherules are of uniform size, shape, and abundance and are interpreted to be sedimentary concretions formed in a near-isotropic groundwater flow regime (*2*, *5*). Spherules are characterized by a volume distribution that is more uniform than random, absence at bedding or other erosional surfaces, multiply fused spherules, and a distinctive composition (>50% Fe_2O_3 as hematite, with Ni/Fe far too low for a meteoritic origin). Neither accretionary lapilli nor oxidized metallic iron impact spherules, which might be other ways of creating small spherules (*17*), would plausibly have these characteristics.

As Opportunity traversed southward from Vostok crater to Olympia, the concretions became notably smaller (≤2 mm), more numerous, and more irregular in shape (Fig. 4B). The increase in number and decrease in size of concretions could reflect an increase in the nucleation rate of hematite or its precursor. Nucleation rates of iron oxides are strongly controlled by the degree of supersaturation with respect to the precipitating mineral phase (*29*, *30*), so an increase in the number of concretions could result from a sudden generation of supersaturated conditions caused by changes in the chemistry of the diagenetic fluid. South of Olympia, adjacent to Erebus crater, concretions are absent at the resolution of the MI (Fig. 2C), but this appears to be a relatively local, possibly facies-controlled, phenomenon because small concretions reappear in outcrops south of Erebus.

Later modification. Three types of later modification are particularly prominent in the Burns formation (Fig. 5): surface rinds up to several millimeters thick that record surface alteration, erosionally resistant fracture fills that include a cement component, and networks of polygonal fractures.

Rinds differ chemically from subjacent outcrop, notably showing enrichment of Na and Cl and depletion of S. They are particularly well developed where they have formed at the interface between outcrop surfaces and thin coverings of soils. This observation suggests that the rind formation process may be ubiquitous and ongoing on exposed or thinly covered outcrop surfaces, but that its rate is substantially slower than the eolian sandblasting of soft outcrop rock by saltating grains that is pervasive across the Meridiani plains. In this model, only where rock surfaces have been protected from sandblasting, for example, when buried by a thin veneer of soil and only recently uncovered, is thick rind formation observed.

Fracture fills are erosionally resistant, often vertically oriented features associated with linear fractures of possible impact origin. These features are spectrally distinct from adjacent outcrop but differ chemically only in detail. APXS data indicate that fracture fills contain siliciclastic materials in amounts similar to or slightly greater than nearby outcrop lithologies; the fill is typically slightly enriched in Al and Si and depleted in Mg and S. Unlike rinds, fracture fills show no substantial Na or Cl enrichment. The high abundance of silicates means that the fills are not primarily precipitated, but the absence of basaltic minerals indicates that fractures are not filled by present-day soils. Instead, the close similarity of fracture fill and country rock lithologies suggests that fractures were filled primarily by intraclastic material derived from adjacent outcrops. The limited total volume of alteration rinds and fracture fill indicates very low aggregate rates of fluid flow and chemical weathering during the time since the Meridiani outcrop rocks were deposited.

Polygonal crack systems commonly mark Meridiani outcrop rocks (Figs. 4B and 5, A and B). These three-dimensional crack systems have typical polygon dimensions of ~10 cm and have been observed both on loose boulders within Endurance crater and on exposed bedrock surfaces south of Endurance. Fracture networks on rock surfaces commonly cut across bedding, indicating that the fracturing significantly postdates the deposition process. Because sulfate minerals can undergo substantial volume reduction upon dehydration, the fractures likely resulted from volume reduction during water loss from hydrated sulfate minerals as environmental conditions became more desiccating.

Temporal relations. Key events in the history of Meridiani Planum include the formation of sulfate-rich sand grains by acid sulfate alteration of basalt, deposition of sand grains to form laminated rock, emplacement of the hematite-rich spherules, and other diagenetic events.

Several lines of evidence demonstrate that sulfate-rich sand grains formed before deposition of the outcrop rock seen today. Perhaps the most compelling of these is the compositional gradient at Endurance crater. The observed vertical gradient in the ratio of sulfates to siliciclastics is readily explained by interaction of a sulfate-rich sandstone with groundwater, but it cannot plausibly be explained by any process in which unaltered basaltic sand grains first form laminated outcrop rock and then are chemically altered in place with no groundwater interaction. Also, acid sulfate alteration of the grains that form the outcrop rocks is pervasive along the rover's full traverse, with no less-altered or unaltered zones anywhere, consistent with substantial reworking and mixing after the alteration but unlikely for alteration in place by vapor or small amounts of water.

Additional evidence comes from textural observations. Many hematitic concretions have been sectioned by the RAT and then imaged by the MI, and none preserves relict sand textures in its interior at 30 μm/pixel resolution. This observation requires that sandstone textures within the concretions were obliterated during concretion growth, consistent with sand grains made of soluble sulfates and siliciclastic materials much finer-grained than the sands themselves, but not with sand grains made of basalt. Also, the grains in the Meridiani outcrop are larger and better rounded than windblown basaltic sands on the current surface of Meridiani Planum. The simplest explanation is that the outcrop grains were made of lower-density, less-resistant materials at the time of their transport and emplacement. Geological and geochemical observations thus agree that the acid sulfate alteration of parent basalts invoked to explain Meridiani chemistry took place in an as-yet undiscovered setting before the accumulation of Meridiani sands now observed in outcrop.

It is also clear that the hematitic spherules formed after the acid sulfate alteration of the

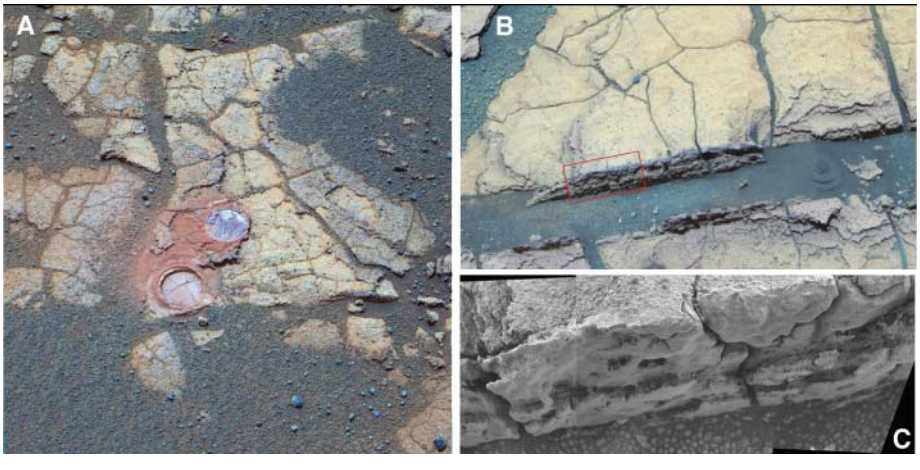

Fig. 5. Evidence of late modification of Meridiani outcrop rocks. (**A**) Pancam false color image of dark rinds atop outcrop rock at Fruit Basket, just north of Erebus crater; round features are RAT holes 4.5 cm in diameter in the rind (upper, Lemon Rind) and subjacent lithology (lower, Strawberry). (**B**) Pancam false-color image of Roosevelt fracture fill along the margin of a linear fracture at Erebus crater. (**C**) Partial MI mosaic ~4 cm wide of the Roosevelt fracture fill, showing mm-scale lamination within the fill; approximate location is shown in red box in (B). Note also the polygonal fracturing of rocks in (A) and (B).

sand grains took place. Sand grains in Meridiani deposits readily recrystallized around spherules (Fig. 2B), which is likely if the grains were sulfate-rich at the time of spherule formation but inconsistent with the sand grains having had a basaltic lithology at that time.

By comparison to eolian deposits on Earth, facies development of the measured section in Endurance crater is interpreted to reflect the interaction between eolian processes and a migrating groundwater table (*6*), with water-deposited beds near the top of the section reflecting aqueous reworking of sands in low-lying areas where ground waters reached the surface. Thus, groundwater infiltration must have begun as Meridiani sands accumulated, not later. The systematic increase in sulfate content observed from the bottom to the top of the measured section may reflect this penecontemporaneous infiltration.

As documented by petrographic textures in MI images, diagenesis ensued after formation of the sand grains and their deposition to form the outcrop: Precipitation of lamina-cutting monoclinic crystals preceded the growth of hematite-rich concretions, which in turn came before the recrystallization of grains, the precipitation of cements around concretions, and the formation of secondary porosity, including the dissolution of earlier formed diagenetic crystals. Diagenesis was largely completed by the time that Meridiani's current geomorphic surface formed; the limited amount of later modification (e.g., rinds, fracture fills, and polygonal fractures) indicates that water has been scarce in the Meridiani region for the past several billion years.

Regional relations. The sulfate-rich deposits examined by Opportunity are located at the top of a several-hundred-meter-thick section of rock that disconformably covers the underlying Noachian cratered terrain (*31*). In fact, the hematite-bearing plains surface materials encountered by Opportunity are dominated by an eolian cover of basaltic sands and lag deposits of hematitic concretions left behind as wind deflated the relatively soft sulfate-rich bedrock. Further, rock exposures to the east, north, and west of the hematite-bearing plains form the etched terrains that extend over several hundred thousand square kilometers (*31*, *32*). These etched-terrain bedrock materials are layered and highly eroded by wind. Analyses of Mars Express OMEGA (Observatoire pour la Mineralogie, l'Eau, les Glaces et l'Activité) data show that the etched terrains have an enhanced 1.92-μm absorption band relative to the Noachian cratered terrain, indicating enhanced abundances of water-bearing mineral phases (*33*). In some areas, kieserite and perhaps polyhydrated sulfate minerals have been identified in etched terrain exposures (*33*, *34*). Thus, Opportunity has examined the top of a widely exposed section of layered deposits that are hydrated and demonstrably sulfate-bearing in multiple locations. This information allows us to consider models for formation of the layered deposits that place rover-based observations into a regional context.

Summary. The first stage in the development of the rocks observed by Opportunity was acid sulfate alteration of basaltic source material to produce sand grains composed of Mg, Ca, and Fe sulfates mixed with a very fine-grained siliciclastic residue. These grains were then reworked by wind in the presence of fluctuating groundwater that occasionally came to the surface and flowed across it. Interaction with substantial amounts of groundwater produced hematite-bearing concretions and a variety of other diagenetic textures, as well as a subsurface gradient in composition at Endurance crater.

None of Opportunity's observations to date reveal the environment in which the sulfate-rich sand grains originally formed. Given the compelling evidence for emergence of groundwaters at Meridiani under generally arid climate conditions, we suggest that the most likely mechanism is that grains originated by erosion from a dirty playa, a pan of sulfate precipitates and fine-grained siliciclastic particles formed by interaction of precursor basalts with acidic groundwaters, followed by evaporation (*2*, *5*, *6*).

In the absence of deposits that have not been reworked by wind and water, other mechanisms for formation of the sand grains, including acid sulfate weathering in a volcanic environment [a component of the scenario suggested by McCollom and Hynek (*16*)], cannot be ruled out. Whatever the formation mechanism, however, it is clear that the grains now observed in outcrop were emplaced by eolian and aqueous processes, and that after their emplacement they interacted with substantial quantities of groundwater.

Although we cannot pinpoint the location where the sand grains formed, we note that there is no need to invoke transport to Meridiani from a distant source region. The eolian and aqueous processes that produced the observed sedimentary facies could have operated exclusively on local scales, so it is plausible that the sulfate-rich sand grains formed at Meridiani, rather than having been transported from elsewhere.

Whatever process produced the sulfate-rich sands at Meridiani, it created enough material to cover several hundred thousand square kilometers. Layered deposits of sulfate minerals have also been found in a number of other areas across the martian surface (*33*). In contrast, hematite has been detected only in a few places on Mars, of which Meridiani is the largest. Because it is the formation of an erosional veneer that renders Merdiani hematite visible from orbit, it may be that other hematite accumulations have thus far escaped detection. But it is also possible that other regions of Mars lacked the specific conditions for groundwater diagenesis responsible for hematite precipitation at Meridiani (*35*).

References and Notes

1. S. W. Squyres *et al.*, *Science* **306**, 1698 (2004).
2. S. W. Squyres *et al.*, *Science* **306**, 1709 (2004).
3. S. W. Squyres, A. H. Knoll, *Earth Planet. Sci. Lett.* **240**, 1 (2005).
4. B. C. Clark *et al.*, *Earth Planet. Sci. Lett.* **240**, 73 (2005).
5. S. M. McLennan *et al.*, *Earth Planet. Sci. Lett.* **240**, 95 (2005).
6. J. P. Grotzinger *et al.*, *Earth Planet. Sci. Lett.* **240**, 11 (2005).
7. J. B. Southard, *J. Sediment. Petrol.* **41**, 903 (1973).
8. J. B. Southard, L. A. Boguchwal, *J. Sediment. Petrol.* **60**, 658 (1990).
9. D. M. Rubin, *Cross-Bedding, Bedforms, and Paleocurrents* (Society of Economic Paleontologists and Mineralogists, Tulsa, OK, 1987).
10. J. F. Bell III *et al.*, *J. Geophys. Res.* **108**, 10.1029/2003JE002070 (2003).
11. D. M. Rubin, *J. Sediment. Petrol.* **57**, 39 (1987).
12. K. E. Herkenhoff *et al.*, *J. Geophys. Res.* **108**, 10.1029/2003JE002076 (2003).
13. R. P. Sharp, *J. Geol.* **71**, 617 (1963).
14. R. E. Hunter, *Sedimentology* **24**, 361 (1977).
15. M. J. Branney, P. Kokelaar, *Pyroclastic Density Currents and the Sedimentation of Ignimbrites* (Geological Society, London, 2002).
16. T. M. McCollom, B. M. Hynek, *Nature* **438**, 1129 (2005).
17. L. P. Knauth, D. M. Burt, K. H. Wohletz, *Nature* **438**, 1123 (2005).
18. G. P. L. Walker, *J. Geol.* **79**, 696 (1971).
19. R. S. L. Sparks, *Sedimentology* **23**, 147 (1976).
20. Sand grain size is commonly evaluated in terms of a φ scale, which presents grain size in powers of 2; a 1-mm grain has a diameter $\varphi = 0$, and a 250-μm grain has $\varphi = 2$. At Meridiani Planum, values of the sorting parameter $\alpha = (\varphi_{84\text{th percentile}} - \varphi_{16\text{th percentile}})/2$ (*17*) are about 0.5, far less than the minimum of 2.0 observed in pyroclastic flow deposits (*17*, *18*).
21. T. S. Ahlbrandt, *U.S. Geol. Surv. Prof. Pap. 1052* (1979), p. 21.
22. S. Gorevan *et al.*, *J. Geophys. Res.* **108**, 10.1029/2003JE002061 (2003).
23. R. Rieder *et al.*, *J. Geophys. Res.* **108**, 10.1029/2003JE002150 (2003).
24. G. Klingelhöfer *et al.*, *Science* **306**, 1740 (2004).
25. P. R. Christensen *et al.*, *J. Geophys. Res.* **108**, 10.1029/2003JE002117 (2003).
26. D. J. Shearman, in *Marine Evaporites*, W. E. Dean, B. C. Schreiber, Eds. (SWPM Short Course No. 4, Oklahoma City, OK, 1978), pp. 6–42.
27. B. C. Schreiber, M. El Tabakh, *Sedimentology* **47** (suppl. 1), 215 (2000).
28. V. M. Gornitz, B. C. Schreiber, *J. Sediment. Petrol.* **51**, 787 (1981).
29. A. C. Lasaga, *Kinetic Theory in the Earth Sciences* (Princeton Univ. Press, Princeton, NJ, 1998).
30. J. F. Banfield, H. Zhang, in *Nanoparticles and the Environment*, J. F. Banfield, A. Navrotsky, Eds. (Mineralogical Society of America, Washington, DC, 2001), vol. 44.
31. B. M. Hynek *et al.*, *J. Geophys. Res.* **107**, 10.1029/2002E001891 (2002).
32. R. E. Arvidson *et al.*, *J. Geophys. Res.* **108**, 10.1029/2002JE0011982 (2003).
33. A. Gendrin *et al.*, *Science* **307**, 1587 (2005); published online 17 February 2005 (10.1126/science.1109087).
34. R. E. Arvidson *et al.*, *Science* **307**, 1591 (2005); published online 17 February 2005 (10.1126/science.1109509).
35. A. H. Knoll *et al.*, *Earth Planet. Sci. Lett.* **240**, 179 (2005).

36. This research was carried out for the Jet Propulsion Laboratory, California Institute of Technology, under a contract with NASA.

Supporting Online Material

www.sciencemag.org/cgi/content/full/313/5792/1403/DC1
Fig. S1

5 June 2006; accepted 28 July 2006
10.1126/science.1130890

Science
AAAS

Two Years at Meridiani Planum: Results from the Opportunity Rover
S. W. Squyres *et al.*
Science **313**, 1403 (2006);
DOI: 10.1126/science.1130890

Science (print ISSN 0036-8075; online ISSN 1095-9203) is published weekly, except the last week in December, by the American Association for the Advancement of Science, 1200 New York Avenue NW, Washington, DC 20005.